Solid State Ionics 1 (1980) 199–210

SILVER IONIC AND ELECTRONIC CONDUCTIVITY IN Ag_9GaS_6

E.E. HELLSTROM * and J. SCHOONMAN
Solid State Chemistry Department, Physics Laboratory, State University of Utrecht, 3508 TA Utrecht, The Netherlands

Received 28 November 1979; in final form 4 January 1980

Electrical measurements on the mixed ionic, electronic conductor Ag_9GaS_6, which undergoes a phase transition at 303 K, were performed. The silver ionic conductivity in the low-temperature α-form measured using an ionic 4-probe method, is given by $\sigma T = 4.3 \times 10^6 \exp[(-29.8\,\text{kJ/mol})/RT]$ S m^{-1} K. The establishment of a fixed, reproducible thermodynamic state in this three-component, single-phase material is discussed. Experiments with Ag_9GaS_6 equilibrated with $Ag + Ag_2S$ and $S + Ag_2S$ revealed n-type conductivity in both equilibrium states. The electronic conductivity of β-Ag_9GaS_6 equilibrated with $Ag + Ag_2S$ is given by $\sigma = 1.2 \times 10^5 \exp[(-30.4\,\text{kJ/mol})/RT]$ S m^{-1}. The electron density and Hall mobility were determined from van der Pauw and Hall effect measurements.

1. Introduction

In a companion paper [1] the high-temperature β-form ($T > 303$ K) of Ag_9GaS_6 was reported to have a high silver ionic conductivity. The ionic conductivity was observed to decrease by a factor of 10^2 on transforming to the low-temperature α-form. This phase is reported to be a mixed ionic, electronic conductor [1], but the electronic conductivity is not reported.

The only additional reference to Ag_9GaS_6 is the original citation by Brandt and Krämer [2] who discovered it in their study of the Ag_2S–Ga_2S_3 join.

In studies of the electrical properties of materials, it is commonly observed that both the electronic and ionic conductivities of a sample are influenced by its preparative and thermal history. This occurs due to the formation of point defects whose concentrations are dependent upon the activity of the different components in the phase. Under conditions of constant temperature and total pressure, two additional parameters need be specified to completely fix the thermodynamics and the defect chemistry of a one-phase, ternary material. For ternary systems the defect

* Present address: Department of Inorganic Chemistry, State University of Utrecht, Utrecht, The Netherlands.

chemistry has been worked out [3–5], while only a few systems have been studied under completely controlled thermodynamic conditions [6].

In this paper it will be shown how the chemical activity of all components in a ternary material are uniquely determined by equilibration with two adjoining phases comprising a three-phase equilibrium-triangle within the ternary system. Electrical conductivity measurements on Ag_9GaS_6 equilibrated with $Ag + Ag_2S$ are presented. Electron concentrations and mobilities extracted from a combination of Hall and van der Pauw measurements are also reported.

The ionic conductivity in α-Ag_9GaS_6 is presented, along with the calculated silver ion mobility and component diffusion coefficient in β-Ag_9GaS_6.

2. Theory

Tubandt and Reinhold [7] observed that at 473 K the electronic conductivity of Ag_2S in equilibrium with Ag was 20 times greater than in equilibrium with S. This is due to a deviation from stoichiometry, i.e. $Ag_{2+\delta}S$, where δ is found experimentally to be positive, corresponding to a silver excess. The Ag and S activities vary continuously across the stoichiometry range of Ag_2S. Since in the high-temperature form of Ag_2S all Ag ions are mobile, and $\delta \ll 2$, the silver ion conductivity is essentially insensitive to variations in Ag stoichiometry at 473 K.

To examine how the defect chemistry can affect the electrical conductivity in ternary phases consider the phase $M_{Ax}M'_{By}X_{A+B}$ which forms from the binary phases M_xX and M'_yX according to

$$A(M_xX) + B(M'_yX) = M_{Ax}M'_{By}X_{A+B} \,. \tag{1}$$

This phase is situated on the tie line joining M_xX and M'_yX as shown in the ternary M–M′–X phase diagram in fig. 1a.

To visualize the possible compositional variations in this phase, the region around $M_{Ax}M'_{By}X_{A+B}$ has been expanded in fig. 1b. The ideal stoichiometry corresponds to a single point, i.e., 6, while the remainder of the one-phase area is the homogeneity region of $M_{Ax}M'_{By}X_{A+B}$. The tie lines of fig. 1a, along which two phases coexist, have expanded to have a finite width in fig. 1b, due to a finite homogeneity in both of the terminal phases.

It must be noted that the point of ideal stoichiometry need not lie in the one-phase homogeneity region. Likewise, the ideal tie lines need not be contained within the two-phase region.

Two compositional variations can occur in a ternary, single-phase sample. Kröger [8] refers to these as a variation in molecularity and a variation in stoichiometry. The former is represented by

$$(A + \delta)(M_xX) + B(M'_yX) = M_{(A+\delta)x}M'_{By}X_{A+B+\delta} \,. \tag{2}$$

An excess δ of M_xX has been added to (or subtracted from) stoichiometric

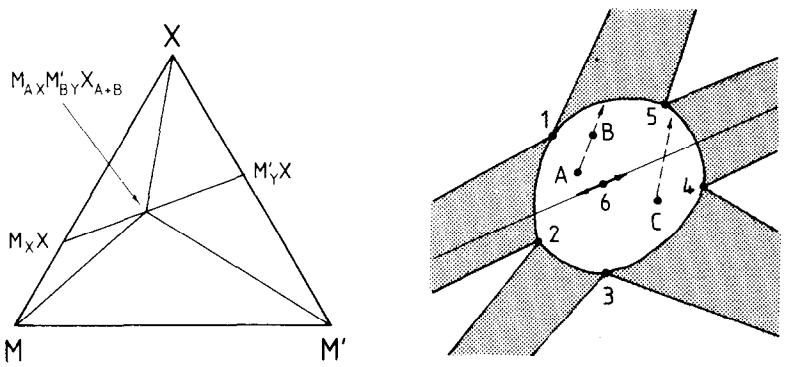

Fig. 1 (a) The ternary system M–M'–X showing the binary phases M_xX, M'_yX, and the ternary phase $M_{Ax}M'_{By}X_{A+B}$. (b) Detail of the ternary phase diagram around the ternary phase $M_{Ax}M'_{By}X_{A+B}$. Three-phase regions are cross hatched and two-phase regions are stipled. Point 6 is the ideal composition $M_{Ax}M'_{By}X_{A+B}$. Solid arrows from 6 show deviations from molecularity along the ideal M_xX–M'_yX tie line. Points 1–5 corresponds to three-phase equilibrium compositions for $M_{Ax}M'_{By}X_{A+B}$. Points A–C illustrate equilibration with component X along the dashed lines, as discussed in the text. For the Ag–Ga–S system, point 6 is Ag_9GaS_6, and points 1 and 2 correspond to Ag_9GaS_6 in equilibrium with S + Ag_2S and Ag + Ag_2S, respectively.

$M_{Ax}M'_{By}X_{A+B}$. This type of variation occurs only along the M_xX–M'_yX tie line, as shown by the arrows in fig. 1b. All other compositions within the one-phase area can only be reached by variations in stoichiometry illustrated below for the incorporation of γ moles of M into stoichiometric $M_{Ax}M'_{By}X_{A+B}$

$$\gamma M + A(M_xX) + B(M'_yX) = M_{Ax+\gamma}M'_{By}X_{A+B} \,. \tag{3}$$

The specific defect equilibria which predominate in any phase depend on the relative formation energies of the different defects, and the prevailing thermodynamic conditions [3–5]. However, if the absolute energy for formation of ionic defects is smaller than that for electronic defects, then the following simplifications apply for deviations from molecularity and stoichiometry.

A variation in molecularity affects the ionic defect concentration, while the number of electronic charge carriers does not change dramatically. However, small changes in the energy bands of the material may occur, leading to variations in the electronic conductivity. The effect on the phases' ionic conductivity depends on the number of charge carriers present at the ideal stoichiometric composition; those phases with low carrier concentrations may be radically affected, while those with high carrier concentrations, such as $RbAg_4I_5$ and Na β-alumina are expected to be only slightly affected.

A variation in stoichiometry affects the ionic defect concentration and also the electronic defect concentration to preserve electroneutrality. Here the variation in both the electronic and ionic conductivity is dependent on the number of charge

carriers present at the ideal stoichiometric composition, as discussed above.

Fig. 1b can be used to illustrate a very common "equilibration" procedure. Consider the formation of a sample of composition A in fig. 1b. To equilibrate A with component X, which is assumed to be a gaseous species, a specified X partial pressure is maintained above the sample. This causes a variation in the X content of the material. This procedure corresponds to moving along the line connecting composition A and pure X (fig. 1b) a distance which depends on the X partial pressure. The composition of the "equilibrated" sample corresponds to point B for instance. The thermodynamics of composition B are completely defined, but its precise composition is not known, and is in general not reproducible. This is easily seen, as in a second preparation of $M_{Ax}M'_{By}X_{A+B}$ a different initial composition C is prepared, due for example to very minor differences in weighing the starting materials. Now by simply equilibrating C with X, i.e. changing the composition along the line connecting C and X, composition B cannot be reproduced.

The tie lines to $M_{Ax}M'_{By}X_{A+B}$ shown in fig. 1a devide the system into five, three-phase regions. Within each of these three-phase regions, at a given temperature and constant total pressure, the thermodynamic state of each phase is fixed. Points 1–5 in fig. 1b correspond to the 5 different, independent, thermodynamically fixed compositions for $M_{Ax}M'_{By}X_{A+B}$ set by the three-phase equilibrium. The composition at these 5 points may not be determinable, but in theory any of these compositions can be achieved by simply equilibrating this phase with the other two appropriate phases.

Weppner and co-workers [9] have given a theoretical treatment for investigating equilibrium conditions within ternary systems using electrochemical techniques. They have applied this technique which reveals those phases coexisting in equilibrium as functions of temperature and composition, to oxides [10].

3. Experimental methods

Ag_9GaS_6 was prepared by zone refining [1].

To determine to which three-phase equilibrium-triangle Ag_9GaS_6 belongs, the EMF of the cell

$$Ag|AgI|Ag, Ag_2S, Ag_9GaS_6 \qquad (I)$$

was monitored as Ag was titrated out of the $Ag + Ag_2S + Ag_9GaS_6$ mixture at 456 K in N_2.

To equilibrate Ag_9GaS_6, cold-pressed pellets were stacked either between cold-pressed pellets of $Ag + Ag_2S$ or $S + Ag_2S$, and heated at 463 K for 12 h in an evacuated quartz tube.

To determine if equilibrium had been established, the EMF of the cell

$$Ag|RbAg_4I_5|Ag_9GaS_6 \qquad (II)$$

(equilibrated as above) was measured as a function of temperature.

Silver ionic conductivity measurements were made using an ionic 4-probe conductivity cell with $Ag|RbAg_4I_5$ electrodes. The Ag_9GaS_6 sample (6 mm diam × 18 mm) was cold pressed (95% dense), and was not thermodynamically equilibrated before the conductivity measurements. Current densities were limited to 3.5 A/m^2. All measurements were done in an N_2 ambient. Temperatures below ambient were achieved using chilled N_2 gas.

Thermoelectric power measurements were carried out using cold-pressed Ag_9GaS_6 samples, either as prepared, or after thermodynamic equilibration. The samples were provided with sputtered Pt electrodes. The measurements were made in air with a maximum ΔT of 20 K.

Two experimental arrangements were employed to measure the electronic conductivity. In the first, an initially nonequilibrated Ag_9GaS_6 pellet was used in the cell

$$Ag, Ag_2S|Ag_9GaS_6|C\,, \tag{III}$$

where C is a graphite electrode. Measurements of the current while varying the potential were made with the graphite electrode both positive and negative. N_2 was used as ambient.

The van der Pauw and Hall effect measurements were performed on a 6 mm diam pellet which had been equilibrated with $Ag + Ag_2S$. Electronic contacts were provided by sputtering 4 Pt pads on one face of the pellet close to the edge, and then soldering Ag lead wires to these Pt pads using In. The current was 0.1 mA and a magnetic flux density of 0.56 kT was used. All measurements were done in a He ambient.

The electronic carrier concentration of a one-carrier system can be extracted from the Hall coefficient R_H using [11]

$$R_H = -(ne)^{-1}\,, \tag{4}$$

where e is the elementary charge and n is the electron carrier density.

4. Results

From the titration experiments with cell I, it was found that Ag_9GaS_6 exists in equilibrium with both $Ag + Ag_2S$ and $S + Ag_2S$. During the titration of Ag out of the right-hand side of cell I, the EMF remained at a plateau of ≈0 mV, then changed continuously to a plateau of ≈200 mV. These plateaus correspond to the three-phase regions $Ag_9GaS_6 + Ag + Ag_2S$ and $Ag_9GaS_6 + S + Ag_2S$, respectively, while the transient corresponds to the two-phase region $Ag_9GaS_6 + Ag_2S$.

EMF measurements with cell II confirmed that the three-phase equilibration technique had indeed established equilibrium in Ag_9GaS_6. At 463 K the Ag activity was $a_{Ag} \approx 10^{-9}$ in Ag_9GaS_6 equilibrated with $S + Ag_2S$, virtually the same value as for equilibrium between $S + Ag_2S$, and $a_{Ag} \approx 1$ in Ag_9GaS_6 equilibrated with $Ag + Ag_2S$.

Table 1
Parameters in Ag_9GaS_6 for different equilibration procedures

Equilibration treatment	ΔWt [a] (w/o)	ΔAg (mol)	ΔEMF (at T_{tr}) [b] (mV)	α at 323 K [c] (mV/K)	$d\alpha/dT$ (mV/K^2)
as prepared	–	–	+4	−0.9	+
Ag + Ag_2S	$+1.1 \times 10^{-3}$	$+1.3 \times 10^{-2}$	+20	−0.48	+
S + Ag_2S	–	–	+50	−0.52	–

a) Average of 6 samples, weight percent (w/o).
b) On cooling, $\beta \rightarrow \alpha$.
c) n-type electronic conductivity.

When equilibrated with Ag + Ag_2S, the Ag_9GaS_6 pellets increased in weight slightly, as given in table 1. The variation in silver stoichiometry, assuming the entire weight change to be due to excess Ag incorporation, is also shown in table 1. Samples of Ag_9GaS_6 equilibrated with S + Ag_2S were found to be saturated with sulfur at room temperature.

On going through the $\alpha \rightleftharpoons \beta$ transition at 303 K the EMF of cell II varied as given in table 1.

As shown in fig. 2, the silver ionic conductivity of Ag_9GaS_6 followed the usual

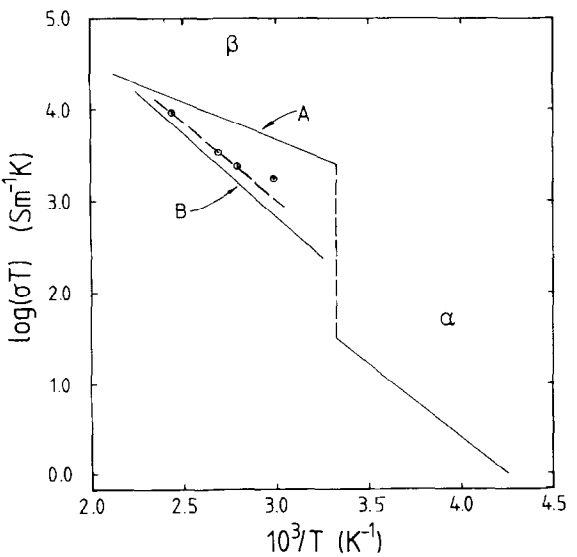

Fig. 2. Silver ionic conductivity (A), and the electronic conductivity measured using cell III (B), and by the van der Pauw technique (○) plotted as $\log(\sigma T)$ versus $1/T$. Electronic conductivity data from cell III are for Ag_9GaS_6 equilibrated with Ag + Ag_2S.

Arrhenius behavior given by

$$\sigma T = \sigma_0 \exp(-\Delta H/RT) , \quad (5)$$

where σ is the conductivity, T the temperature, σ_0 the pre-exponential factor, ΔH the activation enthalpy for conduction, and R the gas constant. In fig. 2, the silver ionic conductivity data are plotted as $\log(\sigma T)$ versus $1/T$. The silver ionic conductivity increases by a factor of 10^2 on transforming to the β-form. The pre-exponentials and activation enthalpies for ionic conduction are given in table 2. Steady-state voltages in the α-form were achieved in 1–5 min, and within 10–60 s in the β-form.

The thermoelectric power results are included in table 1. The thermally induced voltage was linear over the ΔT range, and is reported at the average electrode temperature. For all samples, the hotter electrode was positive, indicating n-type electronic conduction [12].

The electronic conductivity measured with cell III is plotted in fig. 2, for comparison with the ionic conductivity. The pre-exponential factor and activation enthalpy for the electronic conductivity, calculated according to $\sigma = \sigma_0 \exp(-\Delta H/RT)$, are given in table 2. The current–voltage characteristics were ohmic below 20 mV and were identical with the current flowing in both directions.

In cell III, no silver ionic current can flow if a voltage lower than the decomposition voltage of Ag_9GaS_6, i.e. $\approx$200 mV in cell III, is applied with the graphite electrode as anode. Assuming Ag to be the only mobile ion, the steady-state current through the cell is due solely to electronic species. With reversed polarity, both silver ionic and electronic currents can flow.

Since the current–voltage characteristics were independent of the direction of current flow, the current in both directions must be due entirely to electrons. The explanation for this is found from the Tubandt-type measurements described below.

The silver ionic transport number t_{Ag} measured using the Tubandt-type cell

$$Ag, Ag_2S|Ag_9GaS_6|Ag, Ag_2S \quad (IV)$$

Table 2
Pre-exponential factors and activation enthalpies for silver ionic and electronic conductivity in Ag_9GaS_6

Type of conductivity	Form	Temperature range (K)	σ_0 (S m^{-1} K)	σ_0 (S m^{-1})	ΔH (kJ/mol)	Reference
σ_{Ag}	α	233–303	4.3×10^6	–	29.8	this study
σ_{Ag}	β	303–463	1.4×10^6	–	15.9	[1]
σ_e a)	β	303–463	–	1.2×10^5	34.7	this study
σ_e b)	β	–	–	8.8×10^4	28.3	this study

a) Ag_9GaS_6 continuously equilibrated with Ag + Ag_2S (cell III).
b) Measured using the van der Pauw technique.

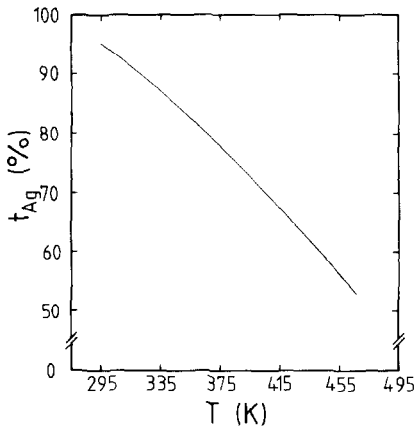

Fig. 3. Silver ionic transport number in Ag_9GaS_6 as a function of temperature, calculated from the data in fig. 2 using eq. (6).

was $t_{Ag} = 0$ at room temperature and 338 K [13]. This indicates that the electronic conductivity is very much higher than the silver ionic conductivity in Ag_9GaS_6. However, this is not valid, as seen in fig. 2. t_{Ag} can also be calculated from

$$t_{Ag} = \sigma_{Ag}/(\sigma_{Ag} + \sigma_{el}) , \tag{6}$$

where σ_{Ag} and σ_{el} are the silver ionic and electronic conductivities, respectively. Plotted in fig. 3 is t_{Ag} for the data of fig. 2 calculated from eq. (6); $t_{Ag} = 0.85$ at 338 K.

Comparing cells III and IV, the Ag, $Ag_2S|Ag_9GaS_6$ interface is common to both. This interface, which in principle should be completely reversible, is not. It allows only electron transfer, indicating a higher charge-transfer overpotential for silver ions than for electrons. The value of $t_{Ag} = 0$ determined from the Tubandt-type measurements is thus for the entire system in cell IV whose characteristics are dominated by the $Ag + Ag_2S|Ag_9GaS_6$ interface. In cell III, it is this same interface which precludes a silver ionic current.

The electronic conductivity determined by the van der Pauw method in a sample equilibrated with $Ag + Ag_2S$ is shown in fig. 2. Above ≈ 430 K, the Pt|In electrodes irreversible converted to blocking contacts.

Hall effect measurements were made on the same sample, and the Hall coefficient is plotted as $\log(R_H)$ versus $1/T$ in fig. 4.

5. Discussion

Ag_9GaS_6 exists in equilibrium with $Ag + Ag_2S$ and $S + Ag_2S$. It is also in equilibrium with $AgGaS_2$ [2], so $Ag_9GaS_6 + AgGaS_2 + S$ coexist in another three-phase

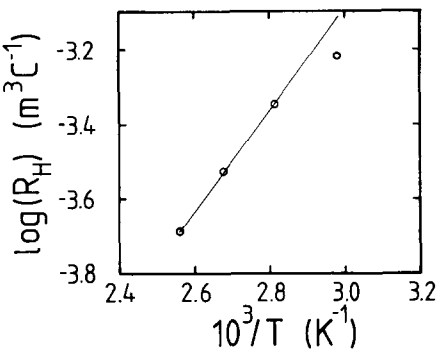

Fig. 4. The Hall coefficient for electrons plotted as $\log(R_H)$ versus $1/T$.

equilibrium-triangle. Phase relations on the Ag side of the Ag_2S–Ga_2S_3 tie line are being studied. Ag_9GaS_6 which was equilibrated with S + Ag_2S was saturated with sulfur due to molton sulfur flowing between the grains of the polycrystalline sample. Further studies with single-crystal samples are therefore required.

The EMF variation on going through the $\alpha \rightleftharpoons \beta$ transformation for Ag_9GaS_6 with the maximum and minimum silver activity indicates that the Ag stoichiometry range in the α-form is slightly wider than in the β-form. This is in contrast to Ag_2S where the high-temperature form is ≈ 40 times wider than the low-temperature form [14].

The thermoelectric power measurements show that the electronic conductivity in Ag_9GaS_6 is n-type over the homogeneity range investigated. In α-Ag_2S, n-type electronic conductivity occurs over the entire existence range, which is found wholly on the Ag-rich side of Ag_2S [15]. The incorporation of excess Ag is given by

$$Ag + V_i^x \rightarrow Ag_i^x \rightarrow Ag_i^{\cdot} + e' \,. \tag{7}$$

Considering the n-type conductivity in Ag_9GaS_6 to be due to incorporation of excess Ag as in eq. (7), then in fig. 1b, both points 1 and 2 lie on the Ag-rich side of the ideal Ag_2S–Ga_2S_3 tie line. From the weight change during equilibration, the separation between points 1 and 2 is estimated to be about 1.3×10^{-2} mol Ag at 463 K.

The structure of Ag_9GaS_6 has not been determined, but in the closely analogous Ag_9GaSe_6 [16,17], there is only a very slight rearrangement of the anions and Ga between the two forms. However, the possible Ag positions, which are essentially geometrically equivalent in both forms, are occupied differently. In the low-temperature form, all the Ag sites are filled, while in the high-temperature form there are more equivalent Ag sites, due to the higher crystallographic symmetry, and these are statistically occupied. The single-crystal X-ray structure determination of high-temperature Ag_9GaSe_6 indicated that all the Ag is mobile [17]. Therefore, all Ag are assumed to be mobile in the β-Ag_9GaS_6 analog.

Using the total volume concentration of Ag (2.9×10^{28} m^{-3}) the silver mobility

and silver component diffusion coefficient for β-Ag_9GaS_6 are given by

$$\mu = (3.1 \times 10^{-4}/T)\exp[(-15.9\ \text{kJ/mol})/RT]\ \text{m}^2/\text{Vs} \tag{8}$$

and

$$D_{Ag} = 2.7 \times 10^{-8}\exp[(-15.9\ \text{kJ/mol})/RT]\ \text{m}^2/\text{s}\ . \tag{9}$$

The concept of a molten Ag sublattice in β-Ag_9GaS_6 is valid, particularly at $T > 423$ K where the Ag mobility approaches that of a molten salt, i.e. 10^{-8} m^2/Vs.

As seen in fig. 2, there is close agreement between the electronic conductivity measured with cell III and using the van der Pauw method for $T > 373$ K. This indicates that essentially the same thermodynamic state for Ag_9GaS_6 prevailed for both measurements. In cell III the three phases Ag + Ag_2S + Ag_9GaS_6 were in physical contact, the procedure used to establish thermodynamic equilibrium, and therefore, the Ag_9GaS_6 was equilibrated with Ag + Ag_2S at all temperatures. The van der Pauw sample was equilibrated with Ag + Ag_2S at 463 K, and then isolated from these phases. In this isolated phase the thermodynamic state is no longer defined at the various temperatures other than the equilibration temperature. However, this does not greatly affect the electronic conductivity as there is only a small variation in the results obtained by the van der Pauw technique and with cell III below 373 K. The Hall coefficient is a direct measure of the reciprocal of the carrier concentration, and as seen in fig. 4, the data lie on a straight line for $T > 373$ K.

To make measurements as a function of temperature on a thermodynamically defined, isolated sample such as that required for the van der Pauw or Hall effect measurements, a series of samples equilibrated at different temperatures must be used, with the measurement being performed at the respective equilibration temperature. This point is presently under study.

The electron density extracted from the Hall coefficient data, calculated excluding the low-temperature datum is given by

$$n = 9.5 \times 10^{25}\exp[(-26.1\ \text{kJ/mol})/RT]\ \text{m}^{-3}\ . \tag{10}$$

The activation enthalpy for formation of excess electrons is probably not the band gap energy E_g of Ag_9GaS_6, but more likely is $E_c - E_d$, where E_c is the conduction band energy level and E_d is the silver donor level for ionization of excess silver incorporated according to eq. (7).

The Hall electron mobility μ_H calculated by combining the van der Pauw and Hall effect results, excluding the low-temperature datum, is given by

$$\mu_H = 5.8 \times 10^{-3}\exp[(-2.2\ \text{kJ/mol})/RT]\ \text{m}^2/\text{Vs}\ . \tag{11}$$

The thermoelectric power of the nonisothermal cell

$$\overset{T_1}{\text{Pt}}\ |\ \text{Ag}_9\text{GaS}_6\ |\ \overset{T_2}{\text{Pt}}\ , \tag{V}$$

in which Pt is electronically reversible, but blocking to silver ions, is due to the elec-

tronic species in Ag_9GaS_6 [18]. The thermoelectric power α is given by [19,20]

$$\alpha = \pm(R/F)[\ln(A/n) + B] \,, \tag{12}$$

where + and − refer to holes and electrons respectively, F is Faraday's constant, n is the electronic carrier density, and B is the transport energy. A is given for the approximation of simple spherical conduction bands by

$$A = 2(2\pi|m^*|kT/h^2)^{3/2} \,, \tag{13}$$

where m^* is the effective mass of the electronic carrier, k is Boltzmann's constant, and h is Planck's constant.

The electron density can be extracted from the thermoelectric power measurements using eqs. (12) and (13) after making reasonable assumptions for m^* and B. Using $m^* = 0.22\ m$ [15] and $B = 0.7$ [21] which are valid for α-Ag_2S, the calculated electron density is 2×10^{22} m^{-3} at 323 K in Ag_9GaS_6 equilibrated with Ag + Ag_2S. These assumptions lead to fair agreement with the value of 5.7×10^{21} m^{-3} from eq. (10).

Wagner [15], and Weppner and Huggins [22] have pointed out that in a phase where the electronic conductivity is equal to, or greater than the ionic conductivity, and the concentration of electronic species is much lower than that of the ionic species, a large enhancement of the ionic diffusion can occur. This enhancement is found to be very high in Ag_2S, Cu_2X(X = S, Se, Te) [15] and in the Li_3M(M = Sb, Bi) intermetallic phases [23]. These same conditions hold in β-Ag_9GaS_6, so an enhancement of the silver ionic conductivity is expected when a silver ionic and electron current flow simultaneously.

6. Summary

Ag_9GaS_6 is a mixed silver ionic, electron conductor. The ionic conductivity in the high-temperature β-form ($T > 303$ K) is quite high, 12 S m^{-1} at 323 K, comparable to the best Ag conductor $RbAg_4I_5$ 30 S m^{-1} at 323 K. On transforming to the low-temperature form, the ionic conductivity decreases by a factor of about 100. In β-Ag_9GaS_6 all the silver ions are mobile, and the silver sublattice can be described as liquid-like. The silver mobility and component diffusion coefficient of the β-form were calculated from the silver ionic conductivity measurements.

In this study, the three-phase equilibration method for reproducibly setting the thermodynamic state of Ag_9GaS_6 was successfully employed. Ag_9GaS_6 which was equilibrated with either Ag + Ag_2S or S + Ag_2S was n-type indicating that Ag_9GaS_6 only exists with a silver excess. The electronic conductivity of Ag_9GaS_6 equilibrated with Ag + Ag_2S was measured. From a combination of van der Pauw and Hall effect measurements, the electron density and Hall mobility were calculated. The electron density was also calculated from the thermoelectric power measurements using values for the effective mass of an electron and the heat of transport of electrons valid for Ag_2S. These two densities agree within a factor of 4.

The density of ionic carriers is much higher than that of the electrons, while the mobility of the silver ions is much lower than that of the electrons in β-Ag_9GaS_6. These are conditions which give rise to a large enhancement of the ionic diffusion, which is expected to occur in β-Ag_9GaS_6.

Acknowledgement

We gratefully acknowledge the assistance of Mr. G.J. Dirksen with preparations of Ag_9GaS_6 by zone refining. We also thank Mr. J.J.M. Binsma for assistance with the van der Pauw and Hall effect measurements which were performed in the Research Institute of Materials at the Catholic University of Nijmegen. One of us (EEH) acknowledges support through a National Science Foundation post doctoral fellowship.

References

[1] E.E. Hellstrom and R.A. Huggins, J. Solid State Chem. 35 (1980), to be published.
[2] G. Brandt and V. Krämer, Mat. Res. Bull. 11 (1976) 1381.
[3] H. Schmalzried and C. Wagner, Z. Physik. Chem. 31 (1962) 198.
[4] H. Schmalzried, Progr. Solid State Chem. 2 (1965) 265.
[5] J.A. Groenink and P.H. Janse, Z. Physik. Chem. NF 110 (1978) 17.
[6] F.A. Kröger, The chemistry of imperfect solids, Vol. 2 (North-Holland, Amsterdam, 1974) tables 20.4 and 21.1.
[7] C. Tubandt and H. Reinhold, Z. Elektrochem. 37 (1931) 589.
[8] F.A. Kröger, The chemistry of imperfect solids, Vol. 2 (North-Holland, Amsterdam, 1974) ch. 20.
[9] W. Weppner, Chen Li-Chuan and W. Piekarczyk, Electrochim. Acta, submitted for publication.
[10] W. Weppner, Chen Li-Chuan and A. Rabenau, Mat. Res. Bull. 13 (1978) 1077.
[11] O. Lindberg, Proc. I.R.E. 40 (1952) 1414.
[12] F.A. Kröger, The chemistry of imperfect solids, Vol. 3 (North-Holland, Amsterdam, 1974) p. 191.
[13] E.E. Hellstrom, unpublished results, Utrecht (1978).
[14] N. Valverde, Z. Physik. Chem. NF 70 (1970) 113.
[15] C. Wagner, J. Chem. Phys. 21 (1953) 1819.
[16] J.-P. Deloume, R. Faure, H. Loiseleur and M. Roubin, Acta Cryst. B34 (1978) 3189.
[17] J.-P. Deloume, Crystal Structure of α-Ag_9GaSe_6, private communication (1979), to be published.
[18] H. Rickert and C. Wagner, Ber. Bunsenges. Physik. Chem. 67 (1963) 621.
[19] J. Bloem, Philips Res. Rept. 11 (1956) 273.
[20] C. Wagner, Progr. Solid State Chem. 7 (1972) 1.
[21] K. Weiss, Ber. Bunsenges. Physik. Chem. 73 (1969) 683.
[22] W. Weppner and R.A. Huggins, J. Electrochem. Soc. 124 (1977) 1569.
[23] W. Weppner and R.A. Huggins, J. Solid State Chem. 22 (1977) 297.